infrastructures

MDPI

Article

Preliminary Assessments of Geotechnical Seismic Isolation Design Properties

Davide Forcellini

Faculty of Civil Engineering, University of San Marino, via Consiglio dei Sessanta, 99, Serravalle 47899, San Marino; davide.forcellini@unirsm.sm

Abstract: This paper proposes a method to investigate the design properties of geotechnical seismic isolation (GSI). This technique has been the object of many research contributions, both experimental and numerical. However, methods that may be used by practitioners for design procedures are still unavailable. The formulation presented herein may be used for preliminary assessments of two important properties: the thickness and the shear wave velocity. Three-dimensional advanced numerical simulations were performed with the state-of-the-art platform OpenSees in order to verify the analytical formulation on a benchmark case study. The elongation ratio has been taken as the relevant parameter to discuss the efficiency of GSI in decoupling the soil from the structure. The main findings consist of assessing the dependency of the elongation ratio on two parameters: the thickness and the shear velocity of the GSI layer. In this regard, a novel formulation was proposed in order to make preliminary design assessments that can be used by practitioners for practical applications.

Keywords: geotechnical seismic isolation; elongation ratio; shear wave velocity; thickness; OpenSees

check for updates

Citation: Forcellini, D. Preliminary Assessments of Geotechnical Seismic Isolation Design Properties. *Infrastructures* **2024**, *9*, 202. https://doi.org/10.3390/infrastructures9110202

Academic Editor: Eugenio Chioccarelli

Received: 11 October 2024
Revised: 2 November 2024
Accepted: 8 November 2024
Published: 11 November 2024

Copyright: © 2024 by the author. Licensee MDPI, Basel, Switzerland. This article is an open access article distributed under the terms and conditions of the Creative Commons Attribution (CC BY) license (https://creativecommons.org/licenses/by/4.0/).

1. Introduction

Geotechnical seismic isolation (GSI) was proposed in 2008 [1] as a low-cost mitigation technique for the earthquake mitigation of structures. The main idea is that GSI can be a valid solution especially for developing countries where the construction of buildings does not provide adequate levels of structural safety during seismic events; such a technique consists of introducing a deformable interface between the soil and the structure [1–4]. In the last 15 years, such a method has been the object of several studies to improve the seismic performance of buildings. In particular, many contributions focused on investigating specialized materials to be applied in the deformable layer with the scope to reduce the seismic forces from the soil to the structures. In this regard, rubber–soil mixtures (RSMs) consist of a composite material with selected properties (such as low shear modulus of RSM), as shown in [5,6]. Other solutions were the object of experimental tests such as stone pebbles [7,8] and low-cost PVC 'sand-wich' (PVC-s) by [9,10], geogrid reinforcements [11], pure tire chip by [12,13] and polyurethane injections [14]. Many materials have been proposed for GSI, such as sand bitumen [15,16], geosynthetics [17,18] and sand–rubber mixtures [19–21].

Many applications were proposed for investigations of the beneficial effects of GSI on structural configurations [22–24] and bridges [25,26]. In particular, the use of tire chips as backfill materials was proposed for retaining structures and bridge abutments [27–31], while EPS geofoam was proposed as a protection for bridge piers [32].

Several techniques that apply GSI principles have been proposed. For example, a subsoil intervention consists of introducing flexible vertical diaphragm walls together with a soft horizontal layer [33,34]. Moreover, horizontal and V-shaped soft buried barriers were also considered as alternative techniques [35,36]. In addition, Ref. [37] proposed the so-called 'Periodic foundation' that consists of concrete and rubber layers to realize effective attenuation zones. In tunnels and pipeline arenas, a soft layer of coating materials was proposed [38,39].

Regarding this background, there is a gap in the literature: numerical modeling and experimental tests are extremely cost-consuming tools and may be performed only at the academic level. This means that the original proposal of a low-cost mitigation technique may be impracticable for common applications and most practitioners need to have easy-to-use design procedures to build up their models. In this regard, the main scope of this paper is to propose a manageable method for design assessments of the properties (such as the thickness and the shear wave velocity of the layer) for preliminary design procedures. The present methodology is derived from the approach proposed for the assessment of the role of soil–structure interaction (SSI) on low-rise buildings [40]; such a methodology consists of considering an equivalent fixed-based system to perform SSI analyses and was validated with non-linear dynamic numerical simulations with OpenSees. In addition, such a methodology was applied in the assessment of the detrimental effects of SSI on the traditional base isolation technique [41,42].

An existing methodology proposed by [43] consists of a lumped-parameter analytical procedure based on equivalent-linear stiffness and viscous damping coefficients along with rocking radiation damping coefficients for surface and embedded foundations. However, the principal limitation of such a methodology consists of the calibration of several coefficients that requires practice and may be particularly time-consuming.

The novelty of the present paper consists of proposing an analytical formulation that considers two main parameters: the thickness and the shear wave velocity of the GSI layer. Thickness has been chosen as the main parameter for representing the geometry of the GSI system and on which the technical cost depends. The shear wave velocity has been chosen to synthetize into a unique parameter the properties of the soil (the shear wave velocity depends on the shear modulus and Poisson ratio). The efficiency of GSI systems depends on the energy dissipation capability and thus on the thickness of the GSI layer, as discussed in [6]. In particular, the GSI layer behaves as a filter and its efficiency may be assessed as the ratio between the accelerations transmitted through to the top of the GSI layer and those measured at the base of the GSI layer. It is worth noting that the thicker the GSI layer is, the more efficient this filter effect becomes. In order to quantify the efficiency of GSI systems, comprehensive experimental and numerical investigations necessarily need to consider the thickness and the mechanical properties of the GSI layer.

In particular, it is demonstrated herein that the dynamic properties of the soil and of the structure are the key parameters for assessing the performance of the GSI layer in terms of period elongation. In addition, the relationship that is herein presented correlates the properties of the soil and of the structure (known during the design procedures) with the unknown characteristics of the GSI layer.

This paper is structured into five sections. The methodology is described in Section 2 by proposing the analytical development of the method. In Section 3, the approach was applied to a case study and numerical simulations were performed to validate the proposed formulation. In Section 4, the obtained results and findings are discussed by considering the practical applications and observations that can be used by practitioners for design purposes.

2. Methods for Design Assessments

The principle of performance-based earthquake engineering design has been considered in the last few decades as the state-of-the-art approach to increase safety against earthquakes via many applications for structures [44,45] and bridges [46,47]. In this paper, this methodology is followed to assess the design properties of the GSI layer. The principal aim is to propose an analytical formulation based on the definition of a three-degrees-of-freedom (3DOF) system that is schematically represented in Figure 1:

DOF1: structure, represented by its mass (m_s), its stiffness (k_s) and its period (T_s);
DOF2: GSI layer, represented by its mass (m_I), its stiffness (k_I) and its period (T_I);
DOF3: soil, represented by its mass (m_g), its stiffness (k_g) and its period (T_g).

It is worth noting that the 3DOF system is not an alternative to the most-advanced numerical simulations. The aim of this method is to make the design procedure of GSI faster by considering two steps.

Step 1

The 3DOF system is used for defining the thickness and the shear wave velocity, by avoiding time- and cost-consuming numerical simulations (such as parametric studies consisting of varying the two parameters) at this preliminary stage.

Step 2.

Once the two parameters have been decided, advanced numerical simulations need to be performed to assess the performance of the system (structure, GSI and soil). However, the number of these simulations will be significantly reduced because of the application of step 1.

In particular, the relationships between the structure and the foundation soil are based on the previous analytical procedure proposed in [40] built up on the definition of two main parameters that synthetize the dynamic properties of the system:

β is the ratio between the structural mass (m_s) and the mass of the foundation soil (m_g):

$$\beta = \frac{m_s}{m_g} \tag{1}$$

α is the squared ratio between the period of the structure (T_s) and that of the soil (T_g), or even the squared ratio between the frequency of the soil (ω_g) and that of the structure (ω_s):

$$\alpha = \left(\frac{T_s}{T_g}\right)^2 = \left(\frac{\omega_g}{\omega_s}\right)^2 \tag{2}$$

It is worth noting that m_s and T_s are the mass and period of the structure, considered fixed at the base (soil–structure interaction (SSI) effects are neglected).

Following the approach described in [48], it is possible to consider the soil as an equivalent 1-DOF system of a H_g and shear wave velocity Vs_g:

$$\omega_g = \frac{\pi Vs_g}{2H} = \sqrt{\frac{k_g}{m_g}} \tag{3}$$

In the same way, assuming that the behavior of the GSI layer can be considered a pure shear-type, it is possible to model it with a 1-DOF system of a H_I and shear wave velocity Vs_I:

$$\omega_I = \frac{\pi Vs_I}{2H_I} \tag{4}$$

Therefore, the coefficient Ω can be defined as the squared ratio between the frequency of the GSI layer and the frequency of the soil:

$$\Omega = \left(\frac{\omega_g}{\omega_I}\right)^2 = \left(\frac{H_I}{H_g}\frac{Vs_g}{Vs_I}\right)^2 \tag{5}$$

in order to account for the two main design parameters of the GSI layer: the thickness (H_I) and the shear wave velocities (Vs_I).

If d and v are the thickness ratio and the shear velocity ratio, which represent the design properties of the GSI layer, they can be defined as follows:

$$d = \frac{H_I}{H_g} \tag{6}$$

$$v = \frac{Vs_I}{Vs_g} \tag{7}$$

We can derive that DOF3 and DOF2 may be condensed in an equivalent single DOF, represented by its frequency (ω_{eq}), its shear velocity (V_{seq}) and its thickness (H_{eq}):

$$\omega_{eq} = \frac{\pi V_{Seq}}{2H_{eq}} = \frac{\pi}{2}\frac{H_g Vs_g + H_I Vs_I}{(H_g + H_I)^2} = \frac{\pi}{2}\frac{Vs_g}{H_g}\frac{(1+d)^2}{1+dv} \quad (8)$$

Therefore, it is possible to calculate the period elongation of the entire system (soil + GSI layer + structure), by applying [40] the following:

$$\frac{T_{SYS}}{T_S} = \frac{\sqrt{2}}{\sqrt{2\alpha + \beta}} \quad (9)$$

where T_{SYS} is the fundamental period of the entire system that elongates due to the presence of both the foundation soil and the GSI layer. As in [20], since the SSI effects are significant when the structural frequency is larger than that of the soil ($m_g >> m_s$), β may be considered zero. Therefore, it is possible to calculate the elongation ratio (e) by introducing (2) inside (9) as follows:

$$e = \frac{T_{SYS}}{T_S} = \frac{1}{\sqrt{\alpha}} = \frac{\omega_s}{\omega_{eq}} = \frac{4}{T_S}\frac{H_g}{Vs_g}\frac{(1+d)^2}{1+dv} \quad (10)$$

It is worth noting that the two variables d and v represent the design properties of the GSI layer, while T_{SYS}, Vs_g and H_g are known quantities.

In the following section, a numerical case study has been performed with different models by applying OpenSees, a state-of-the-art numerical platform for non-linear advanced numerical simulations to validate the method, by verifying Equation (10).

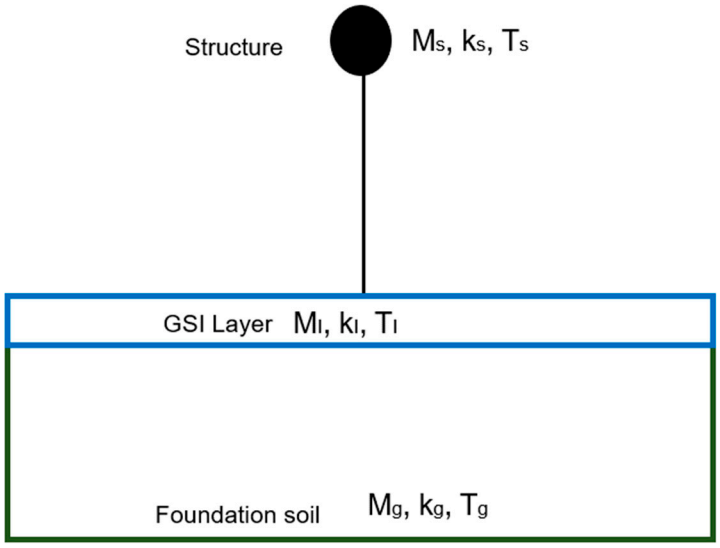

Figure 1. Schematic 3 DOF system.

3. Numerical Case Study

This section presents a numerical case study to validate the proposed formulation. It consists of performing several models of 3D soil–GSI–foundation–structure performed with OpenSees (Figure 2), a state-of-the-art numerical platform for non-linear advanced numerical simulations.

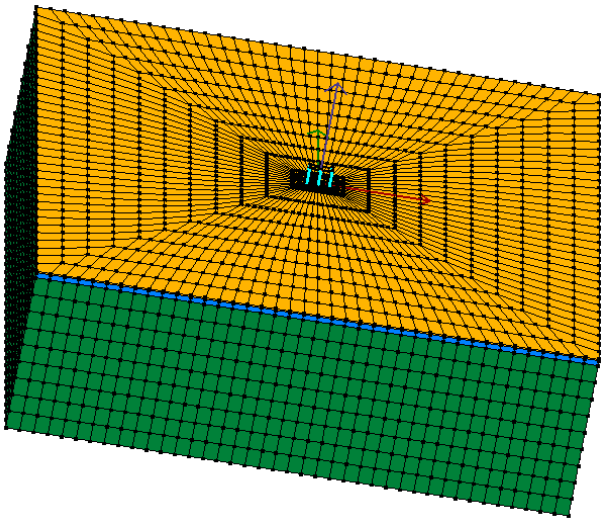

Figure 2. Three-dimensional mesh. Yellow: soil S, blue: GSI layer, green: soil foundation.

The structure represents a benchmark three-floor building (story height: 3.30 m, total height: 9.90 m, longitudinal span: 8 m, transversal span: 6 m) that aims to represent low-rise buildings for those applications GSI is targeting. The structural scheme represents typical residential buildings consisting of vertical columns (fiber section, 0.45 × 0.45 m) and horizontal rigid diaphragms for the floors. Concrete02 (see OpenSees manual [49]) was applied to model the concrete material (core and cover) and the stress–strain relationships are shown in Figures 3 and 4. Steel02 (see OpenSees manual [49]) was used to represent the reinforcement bars (Figure 5). Tables 1 and 2 show the properties adopted for the three materials. In particular, the cover concrete was assumed to lose strength by considering that zero strength is reached in the cover by a strain of 0.006, as applied in [50]. Table 3 shows the dynamic characteristics of the structure in the longitudinal direction.

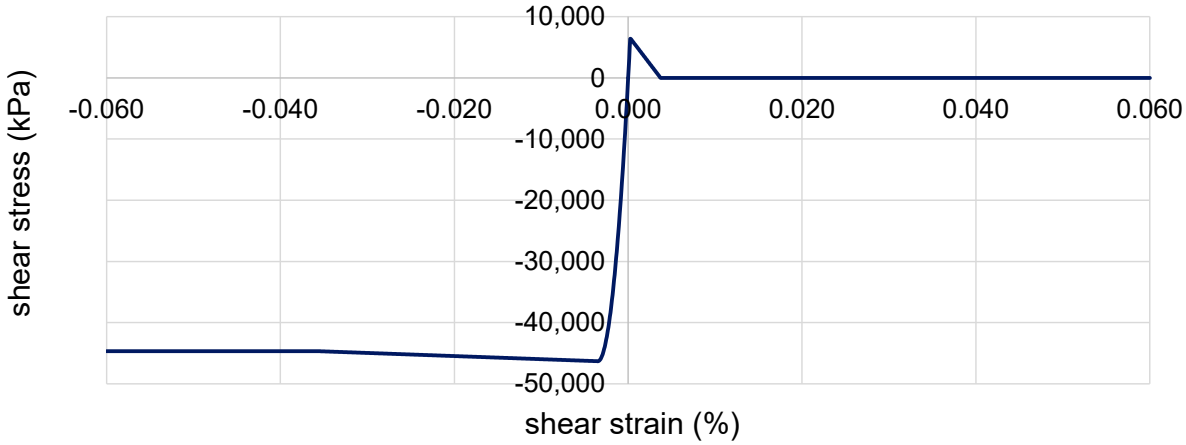

Figure 3. Shear stress–strain relationship Concrete 02 (column core).

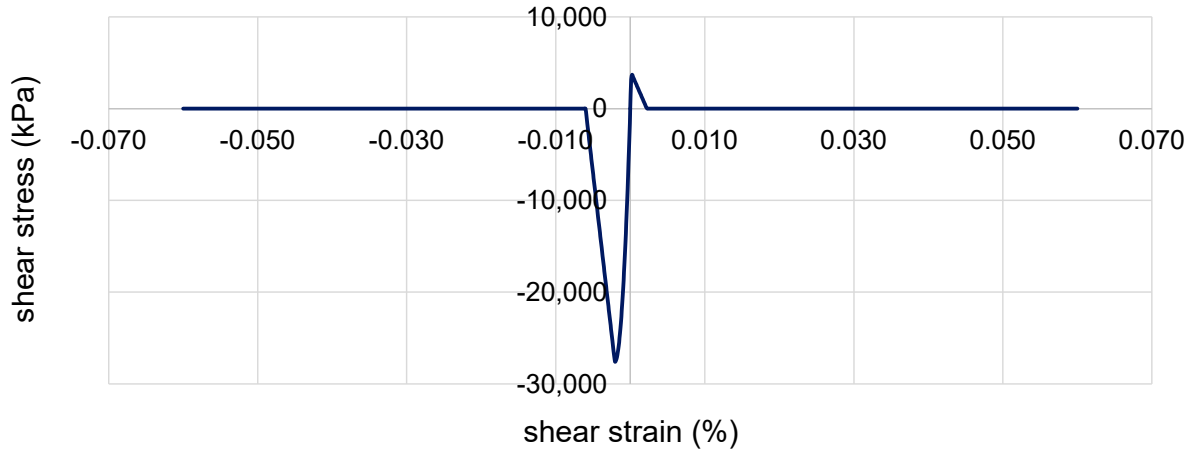

Figure 4. Shear stress–strain relationship Concrete 02 (column cover).

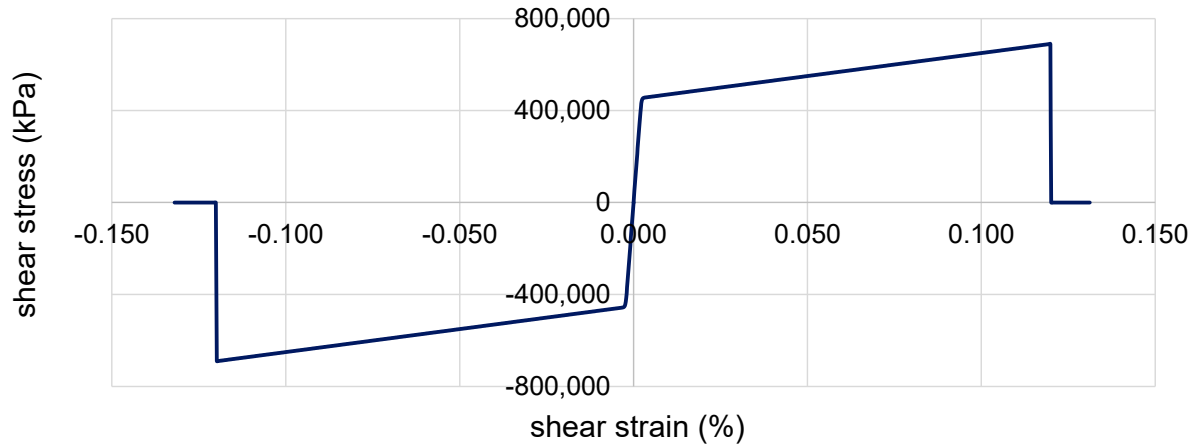

Figure 5. Shear stress–strain relationship Steel 02 (reinforcement bars).

Table 1. Material properties (Concrete 02).

Properties	Core	Cover
Unit weight [kN/m^3]	23.6	23.6
Compressive strength at 28 days [kPa]	−46,304	−27,579
Strain at maximum strength [%]	-3.48×10^{-3}	-2×10^{-3}
Crushing strength [kPa]	−44,660	0
Strain at crushing strength [%]	-3.57×10^{-2}	-6×10^{-3}
Tensile strength [kPa]	6483	3861
Tension softening stiffness [kPa]	1,860,438	1,930,530

Table 2. Material properties (Steel 02).

Properties	
Unit weight [kN/m^3]	77.0
Yield strength [kPa]	455,054
Initial elastic tangent modulus [kPa]	2×10^8
Strain limit [%]	0.12
Strain-hardening ratio	0.02
Controlling parameter R0	15
Controlling parameter R1	0.925
Controlling parameter cR2	0.15

Table 3. Dynamic characteristics of the structure.

T_1 (s)	Mass Participation Ratio (%)	T_2 (s)	Mass Participation Ratio (%)	T_3 (s)	Mass Participation Ratio (%)
0.204	87.24	0.108	7.55	0.075	5.21

The slab foundation was represented by a 0.5 m thick block modeled with Pressure Independent Multi Yield material (density: 24 kN/m^3, shear modulus: 1.25 $\times$ 10^7 kPa, bulk modulus: 1.67 $\times$ 10^7 kPa). In order to reproduce the interaction between the columns and the foundation slab, rigid beam–column links were used to represent the interface, as in [34]. The interaction between the soil and the foundation slab is represented by zero-length elements (see OpenSees manual [49]).

The soil mesh (200 m $\times$ 200 m $\times$ 60 m) was built up with 14,960 non-linear Bbar brick 20-node elements. The 17,220 nodes represent the three degrees of freedom (DOF) and are recorded at the corresponding integration points (see [49]). The boundaries are particularly important for SSI applications and the lateral were herein unconstrained longitudinally in order to model shear deformations, by adopting the penalty method (tolerance: 10^{-4}), as in [41,51]. The base of the mesh was represented with an elastic surface with the aim of representing a small portion of an infinite soil domain. The mesh was calibrated to reproduce the mechanisms of the non-linear deformability of the soil by performing a convergence study between three different meshes with increasing dimensions and number of elements. Mesh dimensions were determined between 0.125 and 0.027 times of the Rayleigh wavelength. The soil domain was discretized with relatively small elements around the structure and gradually larger toward the outer mesh boundaries that were modeled to be impervious, to represent a small section of a presumably infinite soil domain and thus by allowing the seismic energy to be removed from the domain itself. In particular, lateral boundaries were modeled to move in pure shear (free-field conditions), and they were located as far as possible from the structure so as to decrease their effects on the response.

The soil materials (superficial soil (yellow in Figure 2) named soil S, GSI layer (blue in Figure 2) and foundation soil (green in Figure 2), named soil F) were modeled with the Pressure Independent Multi Yield (PIMY) to represent non-linear soil responses (such as hysteretic damping and permanent (plastic) deformations) [52]. Table 4 and Figure 6 show the properties and the backbone curve for soil S and F, respectively. Twenty models were performed with the aim of representing several case studies and verifying Equation (9). In particular, four meshes (M_1, M_2, M_3 and M_4) were built up with different thicknesses: 1 m, 2 m, 3 m and 4 m of GSI layers, respectively. For each of them, five different shear wave velocities (10, 20, 30, 40 and 50 m/s) were considered. Table 5 shows the properties for the GSI layers. Table 6 shows the cases and the results in terms of the elongation ratio (e) for the various cases studies named M_x_y, where x is the value of the thickness and y is the value of the shear wave velocity of the GSI layer. Columns 2 and 3 display the values of v and d, respectively. Column 4 and column 5 show the elongation ratio (e), calculated with (10), and the results obtained with the numerical simulations. Column 6 displays the error between the two approaches (the error varies between -1.2% and +1), demonstrating that Formulation (10) may represent the results. It is worth noting that for thinner cases, Formulation (10) overestimates the results obtained with the numerical simulations. For thicker cases, Formulation (10) is conservative. The errors may be considered due to the assumption that the 3DOF system assumes shear deformation, while the numerical model may consider the non-linear mechanisms inside the soil mesh and thus the results are more accurate. However, as mentioned above, the present approach is not an alternative to numerical simulations, and it can be adopted for preliminary assessments with the aim of avoiding many time- and cost-consuming numerical simulations.

Table 4. Material properties (soils).

Properties	Soil S	Soil F
Unit weight [kN/m^3]	15	18
Shear modulus [kPa]	1.35×10^5	6.48×10^5
Bulk modulus [kPa]	6.3×10^5	3.024×10^6
Cohesion [kPa]	37	75
Shear wave velocity [m/s]	300	600

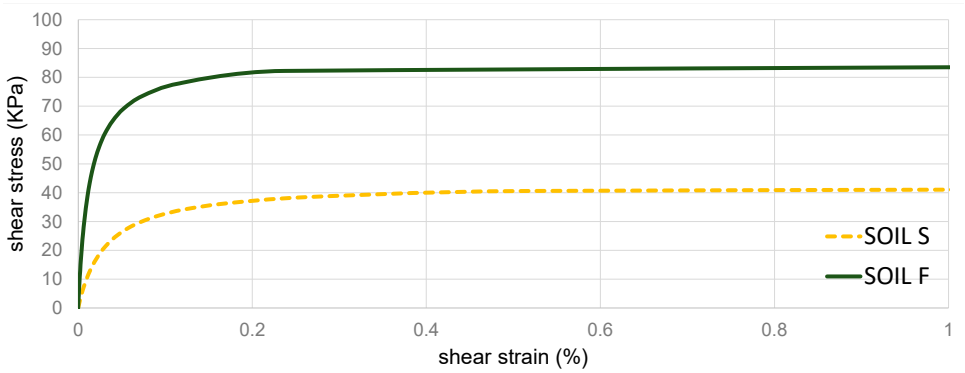

Figure 6. Shear stress–strain relationship (soil S and soil F).

Table 5. Material properties (GSI layers).

Properties	GSI_50	GSI_40	GSI_30	GSI_20	GSI_10
Unit weight [kN/m^3]	15	15	15	15	15
Shear modulus [kPa]	3.75×10^3	2.40×10^3	1.35×10^3	6.00×10^2	1.50×10^2
Bulk modulus [kPa]	1.75×10^4	1.12×10^4	6.30×10^3	2.80×10^3	7.00×10^2
Cohesion [kPa]	37	37	37	37	37
Shear wave velocity [m/s]	50	40	30	20	10

Table 6. Comparison between the elongation ratio resulting from Equation (9): e (10) and the elongation ratio resulting from numerical simulations: e (NS).

	v	d	e (10)	e (NS)	Error
M_1_50	0.0833	0.01667	2.0644	2.0641	−1.2%
M_1_40	0.0667	0.01667	2.0649	2.0647	−1.1%
M_1_30	0.0500	0.01667	2.0655	2.0653	−1.0%
M_1_20	0.0333	0.01667	2.0661	2.0659	−0.8%
M_1_10	0.0167	0.01667	2.0666	2.0665	−0.7%
M_2_50	0.0833	0.03333	2.1296	2.1295	−0.7%
M_2_40	0.0667	0.03333	2.1308	2.1307	−0.6%
M_2_30	0.0500	0.03333	2.1320	2.1319	−0.5%
M_2_20	0.0333	0.03333	2.1332	2.1330	−0.9%
M_2_10	0.0167	0.03333	2.1344	2.1342	−0.8%
M_3_50	0.0833	0.05000	2.1959	2.1960	0.7%
M_3_40	0.0667	0.05000	2.1977	2.1978	0.6%
M_3_30	0.0500	0.05000	2.1995	2.1996	0.4%
M_3_20	0.0333	0.05000	2.2013	2.2015	0.8%
M_3_10	0.0167	0.05000	2.2032	2.2033	0.6%
M_4_50	0.0833	0.06667	2.2630	2.2632	1.0%
M_4_40	0.0667	0.06667	2.2655	2.2657	0.9%
M_4_30	0.0500	0.06667	2.2680	2.2682	0.9%
M_4_20	0.0333	0.06667	2.2705	2.2707	1.0%
M_4_10	0.0167	0.06667	2.2730	2.2733	1.1%

4. Discussion

This section aims to describe the findings presented in Section 2 by proposing a practical discussion of the proposed methodology. In particular, from Equation (10), it is possible to derive the following:

$$\frac{(1+d)^2}{1+dv} = \frac{eT_S V_{sg}}{4H_g} \tag{11}$$

to separate the unknown variables d and v from the known quantities.

Therefore, the design function $\mathcal{F}$ may be considered as follows:

$$\mathcal{F} : F(d,v) = \frac{(1+d)^2}{1+dv} \tag{12}$$

If its partial derivatives are calculated, it is possible to verify that $\mathcal{F}$ increases with d and decreases with v. In other words, there is a direct proportionality with d and an inverse proportionality with v. Therefore, the optimal design would be a compromise between big thickness ratios and small shear velocity ratios. These considerations are particularly important for design purposes since the practitioners may apply (12) to preliminarily estimate the elongation ratio they want to obtain. Then, with an optimization procedure, they can calculate the design variables d and v. By this way, the proposed methodology may significantly speed up the design of GSI if compared with previous procedures or with existing academic outcomes that apply cost-consuming assessments.

In addition, the previous formulation may propose recommendations on the mutual interaction between the stiffness of the soil and the geometric set up of the GSI layer. For example, in the presence of stiff and medium soils, the stiffness of the GSI layer may be considered sufficiently thin and thus economically feasible. However, when the soil is particularly soft, it is opportune to proceed with soil compaction (i.e., air densification), in order to increase the soil stiffness and thus maintain the thickness of the GSI layer at economically feasible values.

Furthermore, the formulation proposed herein may be considered particularly important for developing both green and sustainable applications. For example, layers of rubber–soil mixtures (RSMs) are composed of scrap tires that are available in abundance with an urgent need for recycling. Therefore, the proposed preliminary assessments of GSI techniques may become particularly important for developing countries that do not have the possibility to conduct cost-consuming experimental tests to calibrate the optimal thickness and shear wave velocity. Therefore, the preliminary method may be implemented as a reference design procedure for low-cost applications.

5. Conclusions

This paper investigates the practical design of geotechnical seismic isolation (GSI) layers between the structure and the soil. The main scope is to propose a method that may be used by practitioners for preliminary design assessments. It is worth considering that the approach is not an alternative to more precise but time-consuming investigations. The application prospects are to assist designers in the definition of two variables: the thickness and the shear wave velocity of the GSI layers. The principal aim of the approach is to reduce time- and cost-consuming numerical simulations in the first preliminary stage of the design. The thickness and the shear wave velocity of the GSI layer may be preliminarily assessed in order to guarantee the GSI layer's effectiveness in terms of filtering the seismic accelerations between the soil and the structures. Then, once these two parameters have been designed, the number of necessary advanced numerical simulations will be significantly reduced. The method has been validated with 3D advanced numerical simulations performed by OpenSees with 20 numerical cases on a benchmark system consisting of a low-rise building. The role of the two parameters was discussed to give practical remarks for practitioners in the design procedures of GSI. In addition, the findings may be the first attempt to

implement the GSI technique inside code prescriptions. Future work is needed to test the method with other typologies of structures, such as mid-rise buildings and bridges. Implementing other variables could also be interesting to improve the representativeness of the proposed method.

Funding: This research received no external funding.

Data Availability Statement: Data is contained within the article.

Acknowledgments: The author wants to express his gratitude to Hing Ho Tsang for his encouragement in applying the original 3DOF model to the issue of GSI.

Conflicts of Interest: The authors declare no conflicts of interest.

Abbreviations

m_s	mass of the structure
k_s	stiffness of the structure
T_s	stiffness of the structure
ω_s	frequency of the structure
m_g	mass of the soil
k_g	stiffness of the soil
T_g	stiffness of the soil
ω_g	frequency of the soil
m_I	mass of GSI layer
k_I	stiffness of GSI layer
T_I	stiffness of GSI layer
ω_I	frequency of GSI layer
β	the ratio between the structural mass (ms) and the mass of the foundation soil (mg)
a	the squared ratio between the period of the structure (T_s) and that of the soil (T_g)
H_g	soil thickness
Vs_g	shear wave velocity of the soil
H_I	GSI layer thickness
Vs_g	shear wave velocity of GSI layer
Ω	the squared ratio between the frequency of GSI layer and the frequency of the soil
d	thickness ratio
v	shear velocity ratio
ω_{eq}	frequency of the equivalent soil layer
V_{seq}	shear wave velocity of the equivalent soil layer
H_{eq}	thickness of the equivalent soil layer
T_{SYS}	fundamental period of the entire system (soil + GSI layer + structure)
e	elongation ratio
T_1, T_2, T_3	structural periods (first, second, third)

References

1. Tsang, H.H. Seismic isolation by rubber–soil mixtures for developing countries. *Earthq. Eng. Struct. Dyn.* **2008**, *37*, 283–303. [CrossRef]
2. Tsang, H.H.; Lo, S.H.; Xu, X.; Neaz Sheikh, M. Seismic isolation for low-to-medium-rise buildings using granulated rubber–soil mixtures: Numerical study. *Earthq. Eng. Struct. Dyn.* **2012**, *41*, 2009–2024. [CrossRef]
3. Tsang, H.H. Geotechnical seismic isolation. In *Earthquake Engineering: New Research*; Nova Science Publishers Inc.: New York, NY, USA, 2009; pp. 55–87.
4. Tsang, H.H.; Pitilakis, K. Preface for the special issue on geotechnical seismic isolation (GSI). *Bull. Earthq. Eng.* **2023**, *21*, 3745–3748. [CrossRef]
5. Pitilakis, D.; Anastasiadis, A.; Vratsikidis, A.; Kapouniaris, A.; Massimino, M.R.; Abate, G.; Corsico, S. Large-scale feld testing of geotechnical seismic isolation of structures using gravel-rubber mixtures. *Earthq. Eng. Struct. Dyn.* **2021**, *50*, 2712–2731. [CrossRef]
6. Forcellini, D.; Chiaro, G.; Palermo, A.; Banasiak, L.; Tsang, H. Energy Dissipation Efficiency of Geotechnical Seismic Isolation with Gravel-Rubber Mixtures: Insights from FE Non-Linear Numerical Analysis. *J. Earthq. Eng.* **2024**, *28*, 2422–2439. [CrossRef]
7. Banović, I.; Radnić, J.; Grgić, N. Effectiveness of several low-cost geotechnical seismic isolation methods: A shake-table study. *Bull. Earthq. Eng.* **2023**, *21*, 3923–3947. [CrossRef]

8. Banović, I.; Radnić, J.; Grgić, N. Foundation size effect on the efficiency of seismic base isolation using a layer of stone pebbles. *Earthq. Struct.* **2020**, *19*, 103–111.
9. Tsiavos, A.; Sextos, A.; Stavridis, A.; Dietz, M.; Dihoru, L.; Alexander, N.A. Large-scale experimental investigation of a low-cost PVC 'sand-wich'(PVC-s) seismic isolation for developing countries. *Earthq. Spectra* **2020**, *36*, 1886–1911. [CrossRef]
10. Tsiavos, A.; Sextos, A.; Stavridis, A.; Dietz, M.; Dihoru, L.; Di Michele, F.; Alexander, N.A. Low-cost hybrid design of masonry structures for developing countries: Shaking table tests. *Soil Dyn. Earthq. Eng.* **2021**, *146*, 106675. [CrossRef]
11. Dhanya, J.S.; Boominathan, A.; Banerjee, S. Response of low-rise building with geotechnical seismic isolation system. *Soil Dyn. Earthq. Eng.* **2020**, *136*, 106187. [CrossRef]
12. Hazarika, H.; Pasha, S.M.K.; Ishibashi, I.; Yoshimoto, N.; Kinoshita, T.; Endo, S. Tire-chip reinforced foundation as liquefaction countermeasure for residential buildings. *Soils Found.* **2020**, *60*, 315–326. [CrossRef]
13. Kaneko, T.; Orense, R.P.; Hyodo, M.; Yoshimoto, N. Seismic response characteristics of saturated sand deposits mixed with tire chips. *J. Geotech. Geoenviron. Eng.* **2013**, *139*, 633–643. [CrossRef]
14. Gatto, M.P.A.; Lentini, V.; Castelli, F.; Montrasio, L.; Grassi, D. The use of polyurethane injection as a geotechnical seismic isolation method in large-scale applications: A numerical study. *Geosciences* **2021**, *11*, 201. [CrossRef]
15. Kuvat, A.; Sadoglu, E. Dynamic properties of sand-bitumen mixtures as a geotechnical seismic isolation material. *Soil Dyn. Earthq. Eng.* **2020**, *132*, 106043. [CrossRef]
16. Kuvat, A.; Sadoglu, E.; Zardari, S. Experimental Investigation of Sand–Rubber–Bitumen Mixtures as a Geotechnical Seismic Isolation Material. *Int. J. Geomech.* **2024**, *24*, 04023293. [CrossRef]
17. Nanda, R.P.; Dutta, S.; Das, A.; Khan, H.A. Geosynthetic liner as foundation isolation for seismic protection. *Int. J. Geosynth. Ground Eng.* **2017**, *3*, 21. [CrossRef]
18. Yegian, M.K.; Kadakal, U. Foundation isolation for seismic protection using a smooth synthetic liner. *J. Geotech. Geoenviron. Eng.* **2004**, *130*, 1121–1130. [CrossRef]
19. Kim, H.K.; Santamarina, J.C. Sand–rubber mixtures (large rubber chips). *Can. Geotech. J.* **2008**, *45*, 1457–1466. [CrossRef]
20. Perez, J.L.; Kwok, C.Y.; Senetakis, K. Effect of rubber size on the behaviour of sand-rubber mixtures: A numerical investigation. *Comput. Geotech.* **2016**, *80*, 199–214. [CrossRef]
21. Abate, G.; Fiamingo, A.; Massimino, M.R. An eco-sustainable innovative geotechnical technology for the structures seismic isolation, investigated by FEM parametric analyses. *Bull. Earthq. Eng.* **2023**, *21*, 4851–4875. [CrossRef]
22. Chiaro, G.; Palermo, A.; Banasiak, L.; Tasalloti, A.; Granello, G.; Hernandez, E. Seismic response of low-rise buildings with eco-rubber geotechnical seismic isolation (ERGSI) foundation system: Numerical investigation. *Bull. Earthq. Eng.* **2023**, *21*, 3797–3821. [CrossRef]
23. Dhanya, J.S.; Fouzul, M.A.; Banerjee, S.; Boominathan, A.; Zhussupbekov, A. Shaking table experiments on framed structure resting on geogrid reinforced geotechnical seismic isolation system. *Bull. Earthq. Eng.* **2023**, *21*, 3823–3849. [CrossRef]
24. Edinçliler, A.; Yildiz, Ö. Shaking Table Tests on Geotechnical Seismic Isolation for Medium-Rise Buildings using EPS Beads-Sand Mixtures. *Bull. Earthq. Eng.* **2023**, *21*, 3851–3877. [CrossRef]
25. Forcellini, D.; Alzabeebee, S. Seismic fragility assessment of geotechnical seismic isolation (GSI) for bridge configurations. *Bull. Earthq. Eng.* **2022**, *21*, 3969–3990. [CrossRef]
26. Forcellini, D. Seismic resilience of bridges isolated with traditional and geotechnical seismic isolation (GSI). *Bull. Earthq. Eng.* **2023**, *21*, 3521–3535. [CrossRef]
27. Lee, J.H.; Salgado, R.; Bernal, A.; Lovell, C.W. Shredded tires and rubber-sand as light weight backfill. *J. Geotech. Geoenviron. Eng. ASCE* **1999**, *125*, 132–141. [CrossRef]
28. Hazarika, H.; Kohama, E.; Sugano, T. Underwater shake table tests on waterfront structures protected with tire chips cushion. *J. Geotech. Geoenviron. Eng. ASCE* **2008**, *134*, 1706–1719. [CrossRef]
29. Xiao, M.; Bowen, J.; Graham, M.; Larralde, J. Comparison of seismic responses of geo synthetically reinforced walls with tire-derived aggregates and granular backfills. *J. Mater. Civ. Eng. ASCE* **2012**, *24*, 1368–1377. [CrossRef]
30. Argyroudis, S.; Palaiochorinou, A.; Mitoulis, S.; Pitilakis, D. Use of rubberised backfills for improving the seismic response of integral abutment bridges. *Bull. Earthq. Eng.* **2016**, *14*, 3573–3590. [CrossRef]
31. Mitoulis, S.A.; Palaiochorinou, A.; Georgiadis, I.; Argyroudis, S. Extending the application of integral frame abutment bridges in earthquake-prone areas by using novel isolators of recycled materials. *Earthq. Eng. Struct. Dyn.* **2016**, *45*, 2283–2301. [CrossRef]
32. Karatzia, X.; Mylonakis, G. Geotechnical isolation of pile-supported bridge piers using EPS geofoam. In Proceedings of the 16th World Conference on Earthquake Engineering, Santiago, Chile, 9–13 January 2017.
33. Kirtas, E.; Rovithis, E.; Pitilakis, K. Subsoil interventions effect on structural seismic response. Part I: Validation of numerical simulations. *J. Earthq. Eng.* **2009**, *13*, 155–169.
34. Kirtas, E.; Pitilakis, K. Subsoil interventions effect on structural seismic response. Part II: Parametric investigation. *J. Earthq. Eng.* **2009**, *13*, 328–344. [CrossRef]
35. Nappa, V.; Bilotta, E.; Flora, A.; Madabhushi, S.P.G. Centrifuge modelling of the seismic performance of soft buried barriers. *Bull. Earthq. Eng.* **2016**, *14*, 2881–2901. [CrossRef]
36. Flora, A.; Lombardi, D.; Nappa, V.; Bilotta, E. Numerical analyses of the effectiveness of soft barriers into the soil for the mitigation of seismic risk. *J. Earthq. Eng.* **2018**, *22*, 63–93. [CrossRef]

37. Shi, Z.; Cheng, Z.; Xiang, H. Seismic isolation foundations with effective attenuation zones. *Soil Dyn. Earthq. Eng.* **2014**, *57*, 143–151. [CrossRef]
38. Tsang, H.H.; Lam, J.Y.K.; Yaghmaei-Sabegh, S.; Lo, S.H. Protecting underground tunnel by rubber–soil mixtures. In Proceedings of the 7th International Conference on Lifeline Earthquake Engineering, ASCE-TCLEE, Oakland, CA, USA, 28 June–1 July 2009.
39. Terzi, N.U.; Erenson, C.; Selçuk, M.E. Geotechnical properties of tire-sand mixtures as backfill material for buried pipe installations. *Geomech. Eng.* **2015**, *9*, 447–464. [CrossRef]
40. Forcellini, D. A novel framework to assess soil structure interaction (SSI) effects with equivalent fixed-based models. *Appl. Sci.* **2021**, *11*, 10472. [CrossRef]
41. Forcellini, D. The assessment of the interaction between base isolation (BI) technique and soil structure interaction (SSI) effects with 3D numerical simulations. *Structures* **2023**, *45*, 1452–1460. [CrossRef]
42. Forcellini, D. A 3-DOF system for preliminary assessments of the interaction between base isolation (BI) technique and soil structure interaction (SSI) effects for low-rise buildings. *Structures* **2024**, *59*, 105803. [CrossRef]
43. Tsang, H.-H.; Pitilakis, K. Mechanism of geotechnical seismic isolation system: Analytical modeling. *Soil Dyn. Earthq. Eng.* **2019**, *122*, 171–184. [CrossRef]
44. Alimoradi, A.; Pezeshk, S.; Foley, C.M. Evolutionary seismic design for optimal performance. In *Intelligent Computational Paradigms in Earthquake Engineering*; Chapter 3; Lagaros, N.D., Tsompanakis, Y., Eds.; Idea Group Publishing: Hershey, PA, USA, 2006.
45. Fragiadakis, M.; Lagaros, N.D.; Papadrakakis, M. Performance-based optimum design of steel structures considering life cycle cost. *Struct. Multidiscip. Optim.* **2006**, *32*, 1–11. [CrossRef]
46. Mackie, K.; Lu, J.; Elgamal, A. Performance-based earthquake assessment of bridge systems including ground-foundation interaction. *Soil Dyn. Earthq. Eng.* **2012**, *42*, 184–196. [CrossRef]
47. Zelaschi, C.; De Angelis, G.; Giardi, F.; Forcellini, D.; Monteiro, R.; Papadrakakis, M. Performance based earthquake engineering approach applied to bridges in a road network. In Proceedings of the 5th COMPDYN and ECCOMAS, Crete Island, Greece, 25–27 May 2015; pp. 900–910. [CrossRef]
48. Kramer, S.L. *Geotechnical Earthquake Engineering*; Prentice Hall: Upper Saddle River, NJ, USA, 1996; p. 07458.
49. Mazzoni, S.; McKenna, F.; Scott, M.H.; Fenves, G.L. *Open System for Earthquake Engineering Simulation, User Command-Language Manual*; OpenSees Version 2.0; Pacific Earthquake Engineering Research Center, University of California: Berkeley, CA, USA, 2009; Available online: http://opensees.berkeley.edu/OpenSees/manuals/usermanual/index.html (accessed on 1 October 2024).
50. Mina, D.; Forcellini, D. Soil-structure interaction assessment of the 23 November 1980 Irpinia-Basilicata earthquake. *Geosciences* **2020**, *10*, 152. [CrossRef]
51. Forcellini, D.; Tanganelli, M.; Viti, S. Response site analyses of 3D homogeneous soil models. *Emerg. Sci. J.* **2018**, *2*, 238–250. [CrossRef]
52. Fiamingo, A.; Abate, G.; Chiaro, G.; Massimino, M.R. HS-Small Constitutive Model for Innovative Geomaterials: Effectiveness and Limits. *Int. J. Geomech.* **2024**, *24*, 04024118. [CrossRef]

Disclaimer/Publisher's Note: The statements, opinions and data contained in all publications are solely those of the individual author(s) and contributor(s) and not of MDPI and/or the editor(s). MDPI and/or the editor(s) disclaim responsibility for any injury to people or property resulting from any ideas, methods, instructions or products referred to in the content.